Charge Analysis and Differential Cross-Section Measurements for Large-Angle Argon Ion–Argon Atom Collisions with Energies between 25 and 138 kev*

R. J. CARBONE, E. N. FULS, AND E. EVERHART
Physics Department, University of Connecticut, Storrs, Connecticut
(Received February 23, 1956)

The charge states and differential cross sections of the scattered particles at each angle have been measured for individual collisions between argon ions and argon atoms at large angles. The angular interval ranged from 4 to 20 degrees with a resolution of one degree. Data are presented for several energies between 25 and 138 kev inclusive.

The ion beam traversed a collision chamber which contained the target gas argon. The pressure was maintained low enough to insure that the collision products resulted from two-body interactions, i.e., from single collisions. The scattered particles at each angle passed through a pair of collimating holes and then through an electrostatic analyzer. Percentages in various charge states, ranging from neutral to seven times ionized, were measured. The extent of ionization is found to be a function of the distance of closest approach during the collision in question and not primarily a function of the energy.

The data are also used to determine the absolute differential cross section for scattering of particles. These cross sections are lower than those predicted for simple Coulomb scattering because of the screening effect of the atomic electrons. Agreement is good between the measured cross sections and those calculated from an exponentially screened Coulomb potential.

I. INTRODUCTION

STUDIES of large-angle single collisions between atoms at kev energies are of interest because of the violence of such collisions on an atomic (not nuclear) scale. During the collision the centers of the two atoms may pass within a distance less than the radius of some of the inner electron shells. Under these conditions the collision products are expected to be highly ionized. In this energy range, the velocity of the incident ion is comparable with the orbital velocity of the electrons in the target atom. This condition has been suggested as a criterion for maximum ionization probability.[1]

The large-angle collisions described here are those in which argon atoms, singly ionized, at several energies in the range of 25 to 138 kev, collide with stationary argon atoms. A charge analysis is made of the scattered particles and the differential cross sections measured for angles from 4 to 20 degrees with a resolution of ± 0.5 degree. An earlier paper by two of the present authors[2] has described similar measurements of argon-argon collisions in this energy range and constitutes an introduction to the apparatus and measurements of this paper. However, this earlier work did not include an analysis of the scattered particles.

In addition to the other references cited in our earlier paper,[2] there are two papers by Berry[3] which discuss polar scattering coefficients for collision using argon and neon atomic beams with energies to 7 kev. His experimental data for scattering coefficients are given out to angles as large as 70 degrees, but no charge analysis was attempted.

Single collisions of positive ions with atoms in the energy range of 5 to 30 kev were studied by Fedorenko[4] with an apparatus similar in principle to that used in our experiment. Differential cross sections for various processes are plotted out to 15 degrees for incident ions He^+, N^+, Ne^+, A^+, Kr^+, and others against several noble gas targets. He analyzed the scattered particles for singly, doubly, and triply ionized components, but he did not measure the higher charged components or the neutral component. Fedorenko notes that the scattered particles are generally more highly ionized at the larger scattering angles where the impact parameter is smallest. This reasonable observation is amply illustrated by our data as well.

In the following section the charge analysis of the scattered argon particles is described in detail, and the functional dependence of ionization on various quantities, such as energy, velocity, and distance of closest approach, is studied. The concluding section of this paper discusses the differential cross sections, which are found by using the charge analysis and the absolute scattered currents at each angle. These measured cross sections are compared with those calculated for scattering from an exponentially screened Coulomb potential.

II. CHARGE ANALYSIS

a. Apparatus

The incident beam of singly charged argon ions was furnished by the University of Connecticut heavy ion accelerator. The ions were steered through a small hole into the target gas chamber shown in Fig. 1. This chamber contained the argon target gas at a pressure of about one micron of mercury. No foils were in the path of the beam, and the pressure gradient across the open holes, a and c, was maintained by differential pumping. Details of this and the target gas handling system have been given in our earlier paper.[2]

* This work was sponsored by the Office of Ordnance Research, U. S. Army, through the Watertown Arsenal Laboratories and the Springfield Ordnance District.

[1] H. S. W. Massey and E. H. S. Burhop, *Electronic and Ionic Impact Phenomena* (Oxford University Press, New York, 1952), Chap. VIII.

[2] Everhart, Carbone, and Stone, Phys. Rev. **98**, 1945 (1955).

[3] H. W. Berry, Phys. Rev. **99**, 553 (1955), and **75**, 913 (1949).

[4] N. V. Fedorenko, Zhur. Tekh. Fiz. **24**, 784 (1954).

Along the beam path there are a few particles scattered at large angles. A very small fraction of these particles pass into the solid angle defined by the resolution holes c and d and are then detected.

The entire scattering apparatus was mounted in a large evacuated box. The left side of the target gas chamber, containing the entrance hole a and the connections to the target gas pumps, was held rigid. A flexible bellows allowed the right side, which included the collimating holes and the detecting apparatus, to rotate about an axis through b to any chosen scattering angle θ.

After passing through holes c and d back into the vacuum, the collimated beam of scattered particles passed between the plates of an electrostatic analyzer. The plane lower plate of this analyzer was connected to a positive deflection potential, variable from 0 to 20 kilovolts. The curved upper plate was kept at ground potential. As shown in Fig. 1, the scattered beam is separated by the electric field into its various components. A simple analyzer of this kind will resolve the charge states because all the scattered particles at a given angle have nearly the same mechanical kinetic energy. The energy lost by ionization in the collision is nearly negligible compared to the energy of the particles, which have a large fraction of the energy of the original beam.

There was no focusing of the scattered particles and so the holes in the detectors were made large enough to receive the entire beam despite its spreading. The alignment of the holes in the scattering apparatus to within one-thousandth of an inch was carried out using accurately machined mechanical jigs.

In addition to the primary rotation about the axis through b, the detectors and their associated electrometers could be further rotated about a virtual axis through the point f. This permitted any of the detectors to examine an individual component of the scattered beam in any position.

The Faraday cage, which measured the currents of each charged component, was connected to an electrometer which measured currents between 5×10^{-7} and 5×10^{-16} ampere on several scales. Figure 2 shows the resolved peaks obtained at a scattering angle of 8 degrees and 125-kev incident energy. In this case the Faraday cage was held fixed, and the several charge states were deflected into it by varying the potential on the analyzer.

Additional data were obtained using a secondary electron multiplier. This was the Dumont photomultiplier No. 6365 except that the photosensitive cathode and the glass envelope were removed. The particles to be detected created secondary electrons by colliding directly with the surface of the first dynode. Although this was not an absolute current detector, it was useful for estimating the neutral component as discussed more fully below. In every data set, the analysis made with the Faraday cage was repeated with the secondary electron multiplier.

The thermal detector shown in Fig. 1 was useful at zero angle, but was not sensitive enough to measure the low currents at other angles. The entire apparatus was immersed in a 12-gauss field created by Helmholtz coils; and a small 500-gauss permanent magnet was placed in front of the Faraday cage. The incident and scattered ions had sufficient momentum so that they were not deviated appreciably by these magnetic fields. The fields were for the purpose of preventing extraneous electron currents of the order of 10^{-15} ampere from entering the electrometers.

b. Data

It was necessary to demonstrate that the measured currents were a linear function of the target gas pressure

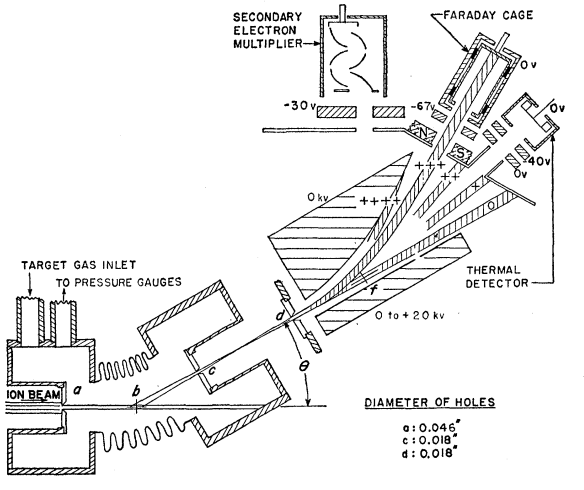

FIG. 1. The scattering apparatus.

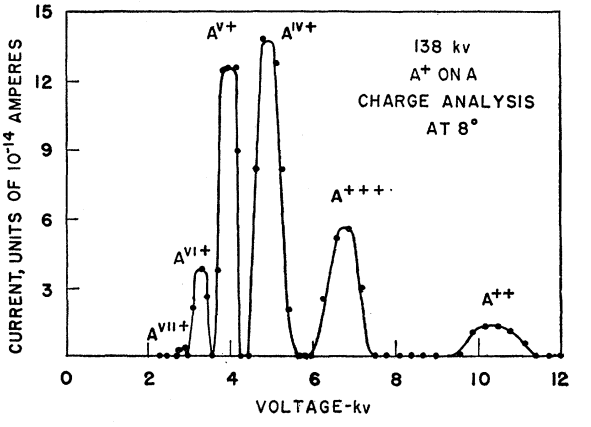

FIG. 2. The current of each charge state as measured with the Faraday cage is plotted *versus* the potential on the electrostatic analyzer. The data were taken at 138 kev and 8 degrees, and show each charge state of the scattered argon between 2 and 7 times ionized.

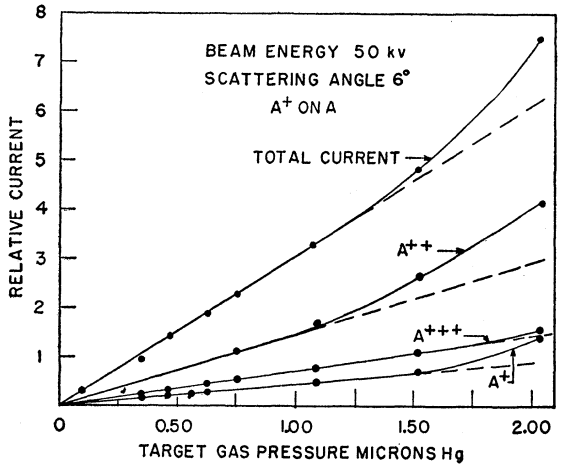

FIG. 3. The ratio of the scattered current of each charge state to the total incident beam current is plotted *versus* the target gas pressure. The data were taken at a scattering angle of 6 degrees and 50-kev incident beam energy. The linear portion of the curves below one micron established the proper pressure region to use for the measurement of single collisions.

to insure that the pressure in the target chamber was low enough to prevent multiple collisions. Figure 3 shows currents obtained at 6 degrees and 50-kev incident energy as a function of pressure. It is seen that the curves are linear below pressures of one micron of mercury at this energy. All of the data were taken between 0.5 and 1.0 micron of mercury.

At each angle, the scattered beam was analyzed to determine the fraction P_n of the particles in each charge state n. The particle current I_n', which is the number of particles per second for the charge state in question, is obtained from the current readings i_n on the Faraday cage by

$$I_n'=i_n/ne, \quad n=1, 2, 3, \cdots, \tag{1}$$

with e being the electronic charge. The particle current of the neutral component I_0' was determined separately with the secondary electron multiplier. This instrument was calibrated for each data set by comparing its output current j_n for each charge state with the corresponding Faraday-cage current. The multiplication factor F, defined as the output current per unit incident particle current, is given by

$$F=nej_n/i_n \tag{2}$$

for the charged components.

This factor was found to be quite independent of n for $n=1, 2, 3, \cdots, 7$, and it was therefore assumed that F had the same value for the neutral components. This is supported by the work of Stier, Barnett, and Evans[5] who showed by direct measurement that this factor had the same value for both charged and neutral particles under conditions similar to our experiment. The neutral particle current is then given by

$$I_0'=j_0/F, \tag{3}$$

and the total particle current at a given angle is thus

$$I'=\sum I_n', \quad n=0, 1, 2, \cdots, \tag{4}$$

from which the fraction in each charge state,

$$P_n=I_n'/I', \tag{5}$$

is obtained.

Currents of 5×10^{-16} ampere which were encountered at large angles were uncertain to possibly one part in five, but most of the currents measured were larger and could be measured with greater accuracy. The over-all accuracy ascribed to the data is $\pm10\%$.

Data are given in Figs. 4 and 5 for argon ion–argon atom collisions at 25, 35, 50, 70, 100, and 138 kev. The ordinate P, is the ratio of particle current of the charge component in question to the total particle current at the given angle θ. Each point on the 25-, 50-, and 100-

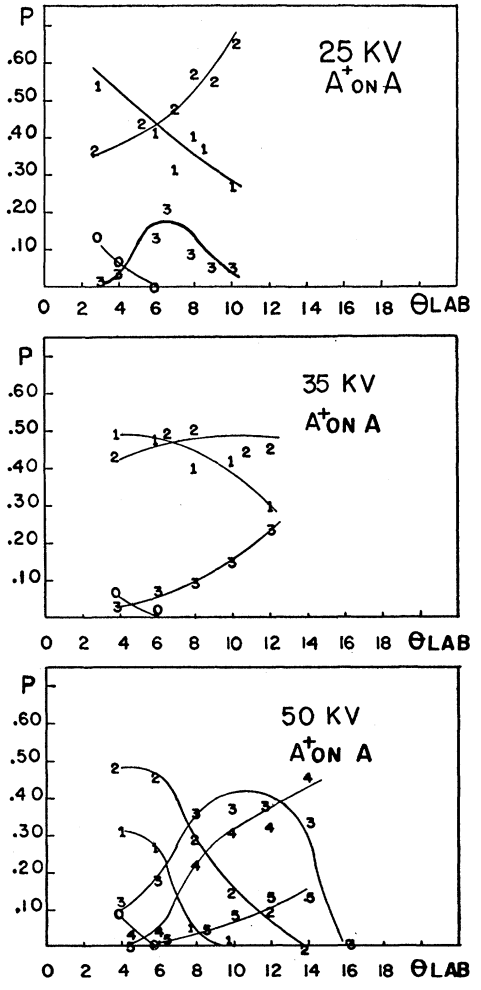

FIG. 4. The observed ionization is plotted *versus* the angle of scattering in the laboratory coordinates at 25-, 35-, and 50-kev incident beam energy. The ordinate P is the ratio of the particle current of each charge state to the total particle current at the angle in question. The points for each charge state are indicated by the appropriate arabic number on the plots. The lines, in this case, are empirical curves through the data.

[5] Stier, Barnett, and Evans, Phys. Rev. **96**, 973 (1954).

kev plots was averaged over several sets of data. The remainder of the plots were for single data sets. Points are indicated as integers which stand for the particular charge state. At the higher energies and larger angles, most of the scattered particles were highly ionized. Over the entire energy range, the neutral component was small and dropped off quickly with increasing angle.

The data were taken at various target gas pressures below one micron of mercury. No variations in the data were observed due to the magnitude of the target gas pressure.

c. Interpretation

The currents reaching the detectors are due to the scattered incident particles, since the cross sections of the recoil particles are negligible in comparison at angles less than 45 degrees.[1]

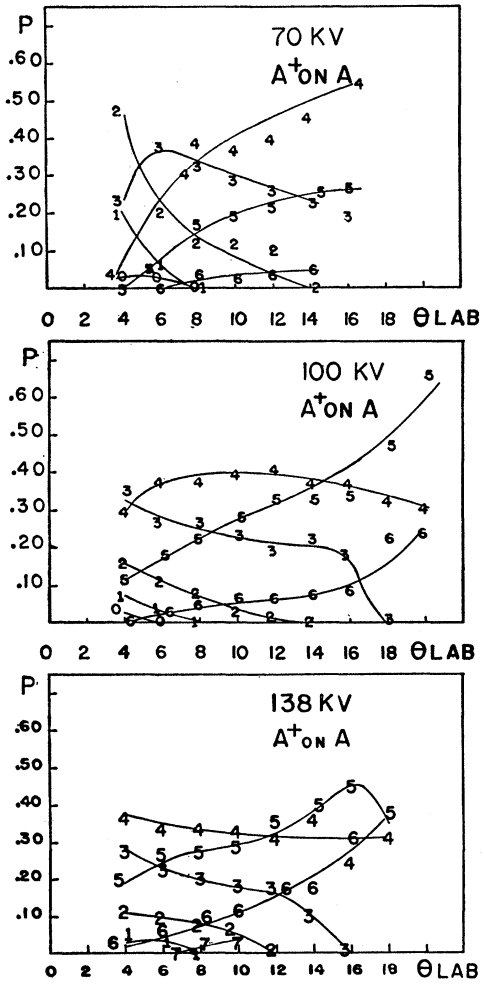

FIG. 5. The observed ionization is plotted *versus* the angle of scattering in the laboratory coordinates at 70, 100, and 138 kev incident beam energy. The ordinate P is the ratio of the particle current of each charge state to the total particle current at the angle in question. The points for each charge state are indicated by the appropriate arabic number on the plots. The lines, in this case, are empirical curves through the data.

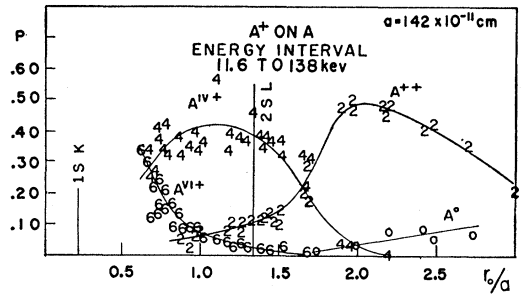

FIG. 6. A plot of P, the ratio of the particle current of each charge state to the total particle current, *versus* r_0/a. Here r_0 is the distance of closest approach in the particular collision and a is the screening radius. The points are for the entire energy range of 11.6 to 138 kev with r_0 being calculated from an exponentially screened Coulomb potential energy function. Only the even charge states are shown on this plot, and they are indicated by their corresponding arabic number. Empirical curves are drawn through the data.

The extent of ionization clearly does not depend on energy or velocity alone since it is found to depend so markedly on the scattering angle as well. The ionization is, however, found to be a function of the distance of closest approach between the centers of the two atoms during the collisions. This distance depends on the potential energy function for the interaction. The function chosen,

$$V(r)=(Z_1Z_2e^2/r)\exp(-r/a), \tag{6}$$

includes the Coulomb potential and an exponential factor which takes into account electron screening. Here Z_1e and Z_2e are the nuclear charges of the colliding particles and a is a screening radius. Bohr[6] has suggested the screening radius given by

$$a=a_0/(Z_1^{\frac{2}{3}}+Z_2^{\frac{2}{3}})^{\frac{1}{2}}, \tag{7}$$

where a_0 equal 0.53×10^{-8} cm and is the radius of the first hydrogen orbit. For argon-argon collisions $Z_1=Z_2=18$ and $a=0.142\times10^{-8}$ cm.

Everhart, Stone, and Carbone[7] have made a detailed classical calculation of scattering from this potential which includes a tabulation of the distance of closest approach r_0 for several energies and all angles. These calculations are in the center-of-mass coordinates and must be converted to laboratory coordinates here.

A number of combinations of energy and angle can give rise to the same value of r_0. For example, r_0 is 0.220×10^{-8} cm for a 125-kev collision which scatters at 4 degrees and it also has the same value for a 25-kev collision at 21 degrees.

For each point of the data the corresponding value of r_0/a has been calculated and the result has been plotted on Fig. 6 for charges of 0, +2, +4, and +6, and on Fig. 7 for charges of +1, +3, +5, and +7. The plotted

[6] N. Bohr, Kgl. Danske Videnskab. Selskab, Mat.-fys. Medd. **18**, 8 (1948). Paragraphs 1.4, 1.5, 1.6, and 2.1 are particularly pertinent to the discussion here.

[7] Everhart, Stone, and Carbone, Phys. Rev. **99**, 1287 (1955).

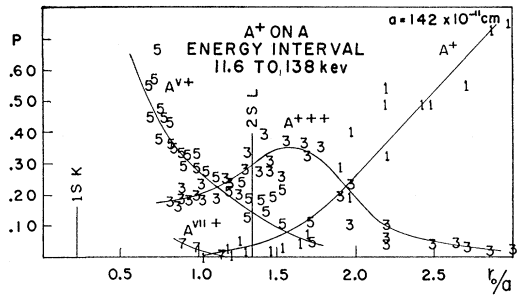

FIG. 7. A plot of P, the ratio of the particle current of each charge state to the total particle current, *versus* r_0/a. Here r_0 is the distance of closest approach in the particular collision and a is the screening radius. The points are for the entire energy range of 11.6 to 138 kev with r_0 being calculated from an exponentially screened Coulomb potential energy function. Only the odd charge states are shown on this plot, and they are indicated by their corresponding arabic number. Empirical curves are drawn through the data.

points are for the entire energy range with many overlapping points that result from different sets of data. Points are also included for data taken at 11.6-kev incident energy. The array of points shows that a strong functional dependence exists for ionization *versus* r_0. The number of electrons removed evidently depends on the depth to which the atoms interpenetrate during the collision. It is interesting to note the positions of the $1s$ K and the $2s$ L shells of argon on the r_0/a axis as shown in the figure. In the most vigorous collisions, the L shell is penetrated but not the K shell.

Plots were also made showing the ionization *versus* the momentum transferred during the collision and showing the ionization *versus* the relative velocity of the ion when it was at r_0. No functional relationship was found to exist in either case, and these plots are therefore omitted. For small angle Rutherford scattering the value of r_0 is inversely proportional to the product of energy U and scattering angle θ. This same relationship holds, at least approximately, for larger angles even with screening taken into account as seen in the numerical example given above. Thus the ionization data, if it were plotted against $U\theta$ instead of r_0, would show a fair dependence on this function as well.

III. DIFFERENTIAL CROSS SECTIONS

The particle differential cross sections are measured for argon ion–argon atom collisions at incident energies of 25, 50, and 100 kev. This quantity is the area of the scattering center for scattering of particles, irrespective of charge, into the angle in question per unit solid angle.

a. Theory of the Measurement

Equation (4) shows how the actual number I' of particles scattered per second through the collimating holes may be determined from the data. This quantity is also given by

$$I'=nN'L\sigma(\theta)\Delta\Omega, \tag{8}$$

where n is the number of target particles per unit volume, N' is the number of incident particles per second, $\sigma(\theta)$ is the particle differential cross section at the angle θ averaged over the effective solid angle of acceptance $\Delta\Omega$, and L is the length of the target volume in the direction of the incident ion beam.

The particle currents I' and N' should not be confused with the corresponding electrical currents I and N which were used in our earlier paper[2] to obtain another differential cross section, that for scattering of positive charge. In particular, the ratio of I' to I would depend on the charge analysis.

The values of L and $\Delta\Omega$ may be found from the geometry of the scattering region as shown in Fig. 8(a). Here δ is the diameter of the incident ion beam. The two collimating holes have the same diameter s. Their distances y_1 and y_2 from the scattering center are especially chosen so that the relationship

$$\delta/s=(y_2+y_1)/(y_2-y_1) \tag{9}$$

is satisfied. Under this condition, the width w of the cone of acceptance at the scattering center is equal to δ and the calculations of both L and $\Delta\Omega$ are simplified.

From the geometry, L is given by

$$L=s\csc\theta(y_2+y_1)/(y_2-y_1)=\delta\csc\theta. \tag{10}$$

The solid angle for scattering varies from a maximum of $(\pi/4)(s/y_2)^2$ over a region near the center of the target volume to zero at the extremes. Figure 8(b) shows the shaded area intercepted at y_2 by the solid angle for an arbitrary position within the target

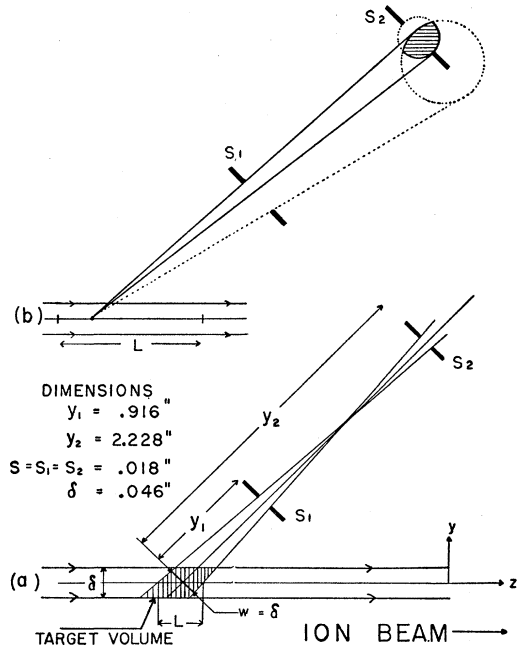

FIG. 8. (a) The scattering region showing the target volume defined by the collimating holes. (b) The solid angle subtended by the collector for an arbitrary point in the target volume.

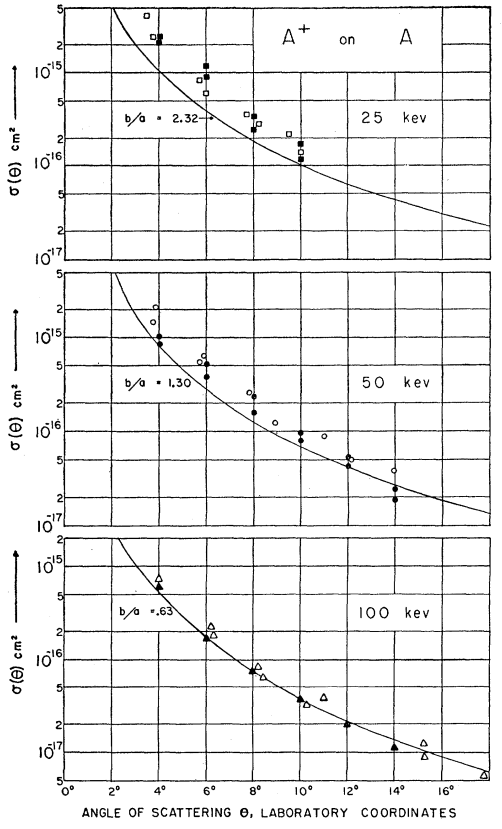

FIG. 9. Differential cross sections in square centimeters for the scattering of particles irrespective of charge for argon ion–argon atom collisions at energies of 25, 50, and 100 kev. The solid points are new data taken at various pressures below 1 micron, and the open points are re-evaluated data computed from a previous experiment performed with different geometry. Differential cross sections, computed for each energy using a screened Coulomb potential energy function, are shown as solid lines, with no adjustment to fit them to the data.

volume. The effective solid angle is found by an integration over the target volume and is given by

$$\Delta\Omega = (2/3)(s/y_2)^2. \tag{11}$$

If one uses Eqs. (8), (10), and (11), the differential cross section is

$$\sigma(\theta) = (3I'y_2^2)/(2N's^2 \csc\theta) \tag{12}$$

for this geometry.

b. Data

Values of θ, n, I', and N' are necessary for obtaining the differential cross section. The first two of these are obtained from measurements of the angle and target gas pressure and temperature as in our earlier paper[2] and I' is found as explained in the section on charge analysis above.

The incident particle current N' was found by multiplying the particle current reaching the detectors set at zero degrees by the ratio of the area of hole a to hole c in Fig. 1. This was necessary since only a portion of the incident beam is intercepted by the collector at zero angle. This compensation assumes the beam to be of uniform density.

An analysis of the argon beam passing through the chamber at zero degrees showed that it was singly charged except for a neutral component which never exceeded 10%. These neutrals were added to the singly ionized particles to obtain the incident particle current. They are attributed to charge exchange processes within the entire length of the scattering chamber. In order to measure single collisions, it would be desirable to operate at pressures so low that less than one percent of the incident beam was altered or scattered inside the chamber. However, if this were done there would not be enough particles scattered at large angles to measure. Thus, a compromise pressure is necessary. When one takes into account the current *versus* pressure data in Fig. 2, this analysis of the incident beam, and the accuracy of calibration of the instruments used, the error assigned to the relative values of the differential cross sections is ±20% and the error assigned to their absolute values is ±50%.

The data are plotted as solid points on Fig. 9 which shows values of $\sigma(\theta)$ in square centimeters plotted against θ for the argon ion–argon atom collisions at the energies noted. The angular resolution is ±0.5 degree.

The open points included on the same figure were obtained from a re-evaluation of previous measurements[2] which were made with a scattering apparatus of different geometry. The previous work measured differential cross sections for the scattering of positive charge as noted above. Using the present analysis of the scattered beam under the same conditions, the differential cross section for scattering of particles was readily obtained. The two sets of data agree within the assigned experimental error.

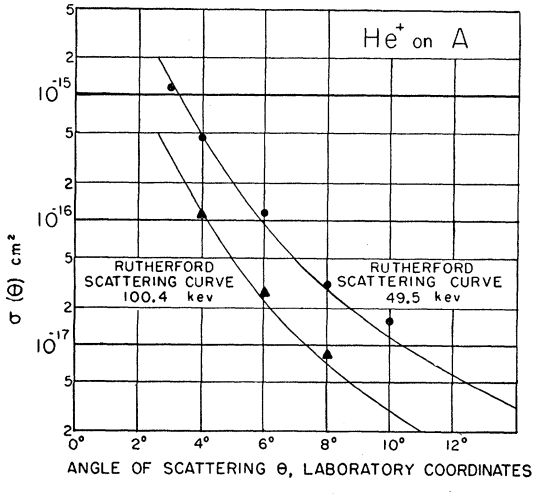

FIG. 10. Measured particle differential cross sections in square centimeters for the single scattering of helium ions on argon atoms at 50 and 100 kev. The Rutherford curves appropriate for each energy have been computed and are shown as solid lines.

c. Comparison of Data with Theory

The solid lines on Fig. 9 show the cross sections computed classically for each energy assuming the screened Coulomb potential given in Eq. (6) with the screening radius a computed from Eq. (7). Details of this calculation are given in the paper by Everhart, Stone, and Carbone[7] which tabulates the values of $\sigma(\theta)/b^2$ in center-of-mass coordinates with the quantity b/a as a parameter. The length b is given by

$$b=Z_1Z_2e^2/U', \tag{13}$$

where Z_1e and Z_2e are the nuclear charges of the colliding atoms and U' is the energy of the collision in center-of-mass coordinates. The value of b/a appropriate to the energy in question is determined, and the tabulated cross section is converted to the laboratory coordinate system. The agreement between the measured cross sections and the calculated curves is excellent at 100 kev and fair at 50 and 25 kev. At these latter energies the calculated curves lie below the experimental points by a factor somewhat in excess of the assigned error of measurement.

In order to test whether there was a systematic error in the measurement or apparatus such as an incorrectly determined solid angle, which would affect the absolute values of the experimental cross sections, a second experiment was performed. Helium ions, singly ionized were scattered from argon gas targets and the particle differential cross sections measured as in the argon experiments. These data are plotted in Fig. 10 for 50- and 100-kev incident energy.

The theory is more certain in this case than for argon-argon collisions, since the corresponding value of b/a is small, and the cross sections can be calculated as for Rutherford scattering with almost no correction needed for electron screening. The solid curves on Fig. 10 are the Rutherford curves and the excellent agreement in this case indicates that there is no excessive systematic error.

PHYSICAL REVIEW VOLUME 102, NUMBER 6 JUNE 15, 1956

Multiple Elastic Scattering in Electron Diffraction by Molecules*

JEAN A. HOERNI
Gates and Crellin Laboratories of Chemistry,† California Institute of Technology, Pasadena, California
(Received November 21, 1955)

Electron diffraction patterns from gas molecules containing heavy atoms can be satisfactorily interpreted in terms of a pseudokinematical theory, in which rigorous atomic scattering amplitudes are used, but the Born approximation is retained for expressing the (molecular) interference between the various atomic contributions. It is shown that the correction brought by the second approximation of the pseudokinematical theory, involving multiple scattering on different atoms, is a smooth function of scattering angle and is therefore unimportant in the study of the oscillating interference term.

I. INTRODUCTION

TWO theories are available for the interpretation of electron scattering by gas molecules. In the kinematical theory one assumes that in the scatterer every infinitesimal element of volume scatters under the influence of the incident electron beam only, and that the total amplitude of the wave diffracted in a given direction is obtained by summing the amplitudes scattered by the various elements of volume, including phase factors due to their different locations. These assumptions are valid as long as the scattered intensity is always much weaker than the intensity of the incident beam. Mathematically, the summation over elements of volume is equivalent to taking the Fourier transform of the electrostatic potential distribution within the scatterer. This is also equivalent to applying the Born approximation to the entire problem.

Recently, it has become apparent[1] that the Born approximation is not valid at the voltages currently used in electron diffraction studies (10–80 kev), even in the case of scattering by a single atom. Let us consider the elastic scattering of electrons of velocity v and wavelength λ by a central potential $V(r)$ due to an atom of atomic number Z. If the amplitude of the spherical scattered wave is written as $f(\theta)e^{ikr}/r$ (where θ is the scattering angle and k is $2\pi/\lambda$), it is found that the atomic scattering amplitude $f(\theta)$ is generally complex, unlike the value $f^B(\theta)$ given by the Born approximation, which takes the real value[2]

$$f^B(\theta)=\frac{2k\alpha}{Ze^2}\int_0^\infty V(r)\frac{\sin br}{br}r^2dr=-\frac{2k\alpha}{b^2}\left(1-\frac{F(\theta)}{Z}\right). \tag{1}$$

Here $\alpha=-Ze^2/\hbar v$, $b=2k\sin\frac{1}{2}\theta$, and the x-ray form factor $F(\theta)$ is the Fourier transform of the electronic

* This work was supported by the Office of Naval Research. Reproduction in whole or in part is permitted for any purpose of the U. S. Government.
† Contribution No. 2055.

[1] V. Schomaker and R. Glauber, Nature **170**, 290 (1952).
[2] Z. G. Pinsker, *Electron Diffraction* (Butterworths Publications, London, 1953), Chap. 7.